STRING STABILITY ASSESSMENT OF FOLLOWERSTOPPER AS WAVE-DAMPENING CONTROLLER FOR MIXED-AUTONOMY

Md Nazmus Shakib
AI, Autonomy, Resilience, Control Lab (AARC Lab)
Department of Electrical & Computer Engineering
The University of Alabama in Huntsville, USA
ms0393@uah.edu

Md Shihab Uddin
AI, Autonomy, Resilience, Control Lab (AARC Lab)
Department of Electrical & Computer Engineering
The University of Alabama in Huntsville, USA
mu0018@uah.edu

Rahul Bhadani, Ph.D., Corresponding Author
AI, Autonomy, Resilience, Control Lab (AARC Lab)
Department of Electrical & Computer Engineering
The University of Alabama in Huntsville, USA
rahul.bhadani@uah.edu

Word Count: 5116 words + 0 table(s) $\times$ 250 = 5116 words

Submission Date: August 1, 2025

ABSTRACT

This study evaluates the string stability of the Followerstopper (FS) controller, a known wave-dampening adaptive cruise control algorithm, in an eight-vehicle platoon scenario. An eight-vehicle platoon (one human-driven leader and seven automated followers) is simulated using a real-world leader speed profile, implemented in both a microscopic traffic simulator SUMO and a high-fidelity physics-engine simulator CARLA. We employ a time-domain evaluation framework with metrics such as head-to-tail velocity amplification, $\mathscr{L}_2$-norm disturbance attenuation, relative speed differences, and spacing error. Results show that the FS controller nearly eliminates disturbance amplification: the head-to-tail amplification factor is approximately 0.994 in both SUMO and CARLA, indicating slight attenuation of the leader's perturbations. The disturbance "energy" (quantified via the $\mathscr{L}_2$ norm of speed errors) decreases downstream, and once the FS is activated, large relative speed oscillations and spacing deviations are rapidly damped. These improvements are consistent across both simulators, which demonstrates robust performance of FS under realistic vehicle dynamics. The proposed time-domain-based string stability assessment in realistic mixed-autonomy settings indicates that Followerstopper effectively stabilizes traffic flow by dissipating disturbances in platoon formation.

Keywords: Mixed-autonomy, Control Systems, Intelligent Transportation, Followerstopper, String stability

INTRODUCTION

We have seen rapid progress in vehicle technologies over the years, in a way that vehicles are now computers on wheels. Such development has created a pathway for full vehicle automation (Level 5) on roadways where the future envisions end-to-end driving without human intervention (*1*). Such a scenario promises a safer driving experience, fewer accidents, increased fuel efficiency, reduced travel time, and economic advantage (*2*). However, before level 5 automation can be achieved, vehicle technology has to transition through a mixed-autonomy scenario (*3*) where only some vehicles are automated, yet not fully autonomous; most will still be level 2-4. Nevertheless, there is a proliferation of advanced driver assistance systems (ADAS) such as adaptive cruise control (ACC), lane-keep assist (LKA), collision warning systems, etc. (*4–7*). Experiments have shown that such automation can be used for phantom traffic jam mitigation in a mixed autonomy scenario by actuating a few percent of vehicles in the traffic (*8–11*). One such scenario that we study in this research is the connected & automated vehicles (CAVs) scenario, where a platoon of vehicles can be deployed to stabilize the traffic on the freeway.

In this work, we study the string stability analysis of a wave-dampening controller, Follower-stopper (*8, 9, 12*), that was deployed in a ring-road experiment to demonstrate that even a single vehicle with an appropriately designed autonomous control law can stabilize the traffic wave to a significant extent. Although the prior work addressed the wave-dissipation ability of Follower-stopper in an experimental ring-road setup under low-speed (< 9m/s) conditions, the behavior of a Followerstopper-controlled platoon of vehicles is unexplored. In this context, we are interested in exploring the stability of a Followerstopper-controlled platoon of vehicles. In a platoon, if a vehicle's speed oscillates, such an oscillation will tend to pass to the following vehicles along the downstream traffic. To avoid a phantom traffic jam in such a scenario, we desire that the amplitude of such speed oscillations decay as they travel along the platoon. If a small perturbation in the leading vehicle of the platoon is amplified as it progresses along the platoon towards the following vehicles, the following vehicles eventually need to stop to avoid a collision, causing traffic jams.

When compared to human-driven vehicles (HVs), a controlled platoon of vehicles offers the advantage of reducing intervehicle spacing (*13*). A tight platoon can provide reduced traffic congestion on the freeway, saving fuel consumption and overall making traffic more efficient. If we look at the literature, we find several different ways to define string stability of a platoon; some are more relaxed than others. The main question this research work tries to address is whether a Lagrangian controller that has been shown to reduce phantom jams and stabilize traffic at low speeds is equally capable of stabilizing traffic when deployed as a cooperative adaptive cruise control (CACC). The main contribution of this work is as follows. We describe the Followerstopper controller model as a CACC for a platoon of vehicles following a leader vehicle with a speed profile representative of human drivers. Simulation is conducted at a varying level of fidelity, namely, discrete-event simulation using SUMO (*14*), and physics-engine-based simulation with CARLA (*15*). Such a simulation strategy ensures that our findings are not merely artifacts of simulation but represent real-world deployment scenarios in lieu of field experiments.

BACKGROUND

Theoretically, and in simulation, CACC models have been studied extensively for their properties such as closed-loop string stability, ability to dampen phantom traffic jams (*13*), stability,

the impact on fuel efficiency, and their ability to influence the traffic flow in mixed autonomy settings (*16*). Interest in the mixed-autonomy traffic has grown since the Arizona Ring-road Experiment (*8*). In a mixed-autonomy traffic, it is expected that only a few percent of vehicles are automated (see Figure 1).

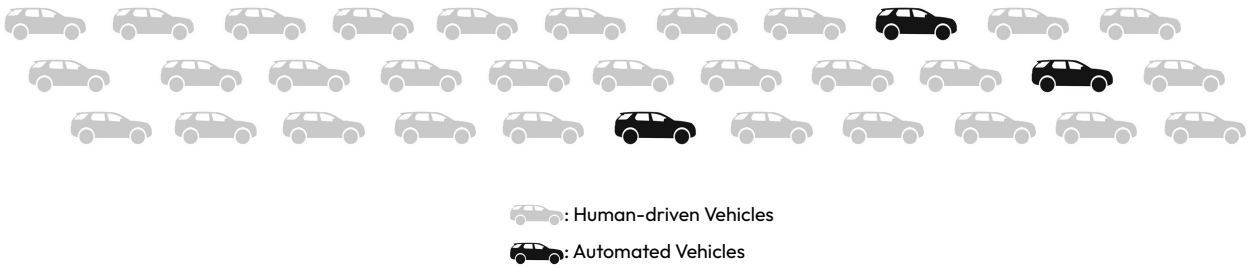

FIGURE 1: A mixed-autonomy scenario where only a few vehicles are highly-automated.

In addition, such automation can vary from Level 2 to Level 5. As of the writing of this article, there are rarely any Level 5 automated vehicles on the freeway in operation. However, in limited capacity, many companies such as Waymo, Baidu, WeRide, and Pony.ai are testing their Level 5 automation through robotaxi geo-fenced to certain regions within some cities. Sugiyama, in his seminal work (*17*), showed that traffic jams can occur without any bottlenecks under naturalistic human driving. In Tucson, Arizona, Stern et al. later demonstrated experimentally on a circular test track that a small fraction of vehicles, operated as Lagrangian actuators, can actively dissipate stop-and-go waves. (*8*). Vehicles, acting as Lagrangian actuators, were autonomously controlled by the Followerstopper controller (*9*). However, as we note that the prevalence of vehicle-to-vehicle communication is not significant in practice, we pose the question: are Lagrangian actuators that can dissipate stop-and-go traffic waves string-stable and can form a stable platoon? We address the research questions through two complementary, stand-alone simulation studies. First, we use SUMO, a discrete-event simulator that treats vehicles as point masses; its computational efficiency allows us to generate large traffic volumes and test scenarios quickly. We also employ CARLA, which runs on the Unreal Engine and models vehicles as rigid bodies with full dynamics. CARLA supports the OpenDRIVE format for road-network import and provides a high-fidelity environment that represents real-world vehicle behavior more accurately.

The rest of the paper is organized as follows

TODO: add organization later

PROBLEM SETUP

We consider a homogeneous string of $n+1$ identical vehicles with a lead vehicle, indexed $i = 0$, having an exogenous input (human driver). The first automated vehicle in the platoon starts with index $i = 1$. Each follower i measures the relative distance $\Delta x_i(t) = x_{i-1}(t) - x_i(t) - L$ and $\Delta v_i(t) = v_{i-1}(t) - v_i(t)$. L is the length of each vehicle, $x_i(t)$ is the position of i-th vehicle, $v_i t$ is the velocity of each vehicle at timestamp t. We also assume error-free, lossless communication where each vehicle has full information about other vehicles in the platoon. In addition, we also assume that the first vehicle in the platoon has sensing capabilities to measure the relative distance and relative

speed of the leader vehicle. This assumption is necessary as we do not assume any communication between human-driven vehicles and automated vehicles. Overall setup is provided in Figure 2 While the SUMO simulation provides ideal conditions, actuation lag in the CARLA simulation is

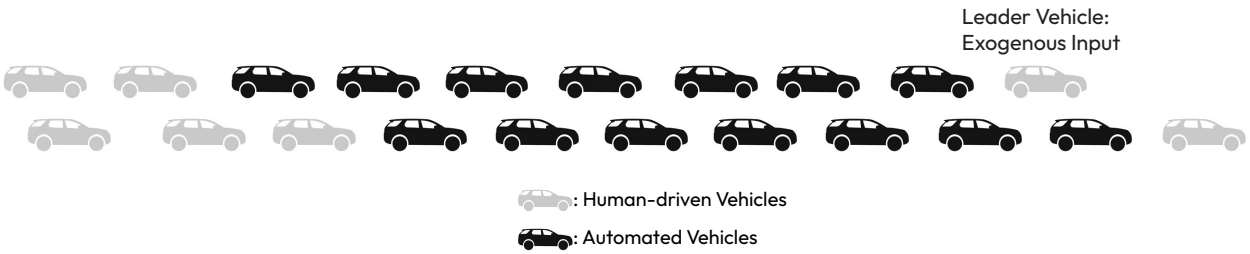

FIGURE 2: Platooning in the traffic flow

handled as an artifact of the complex simulation environment. In this work, we do not address any other imperfect condition either in estimation or in inter-vehicle communication. In addition, no lane change scenario is considered in our use cases.

Controller Structure

Followerstopper controller is a car-following strategy designed to suppress stop-and-go traffic waves by adjusting the ego vehicle's speed based on its relative distance and velocity to the leading vehicle (*9, 12*). It operates in multiple control zones based on a phase-space representation of the traffic state, where the ego vehicle transitions smoothly between stopping, adaptation, and the safety region.

The control law for vehicle i driven using Followerstopper can be written as

$$v_{\text{cmd},i}(t) = f_{\text{FS}}(\Delta x_i(t), \Delta v_i(t), v_{i-1}(t)) = \begin{cases} 0, & \text{if}(\Delta x_i, \Delta v_i) \in \mathscr{S}_1 \\ v(v_{i-1})\frac{\Delta x_i - d_1(t)}{d_2(t) - d_1(t)}, & \text{if}(\Delta x_i, \Delta v_i) \in \mathscr{S}_2 \\ v(v_{i-1}) + (r - v(v_{i-1}))\frac{\Delta x_i - d_2(t)}{d_3(t) - d_2(t)}, & \text{if}(\Delta x_i, \Delta v_i) \in \mathscr{S}_3 \\ r_i, & \text{if}(\Delta x_i, \Delta v_i) \in \mathscr{S}_4 \end{cases} \tag{1}$$

where $v : \mathbb{R} \to \mathbb{R}$ is $v(v_{i-1}) = \min\{\max\{v_{i-1}, 0\}, r_i\}$. Four sets $\mathscr{S}_1$, $\mathscr{S}_2$, $\mathscr{S}_3$, and $\mathscr{S}_4$ divided by three safety envelopes as are defined below:

$$\begin{aligned} \mathscr{S}_1 &= \left\{(\Delta x_i, \Delta v_i) \in \mathbb{R}^2 | 0 < \Delta x_i \leq d_1(\Delta v_i)\right\}, \\ \mathscr{S}_2 &= \left\{(\Delta x_i, \Delta v_i) \in \mathbb{R}^2 | d_1(\Delta v_i) < \Delta x_i \leq d_2(\Delta v_i)\right\}, \\ \mathscr{S}_3 &= \left\{(\Delta x_i, \Delta v_i) \in \mathbb{R}^2 | d_2(\Delta v_i) < \Delta x_i \leq d_3(\Delta v_i)\right\}, \\ \mathscr{S}_4 &= \left\{(\Delta x_i, \Delta v_i) \in \mathbb{R}^2 | d_3(\Delta v_i) < \Delta x_i\right\}. \end{aligned} \tag{2}$$

and switching boundary $d_j : \mathbb{R} \to \mathbb{R}$ are:

$$d_j(\Delta v_i) = \omega_j + \frac{1}{2\alpha_j}\min\{0, \Delta v_i\}^2, \quad j = 1, 2, 3, \tag{3}$$

where $\omega_1 = 4.5$, $\omega_2 = 5.25$, $\omega_3 = 6.0$, $\alpha_1 = 1.5$, $\alpha_2 = 1$, $\alpha_3 = 0.5$. Through our controller design, we control the velocity of the Lagrangian control vehicle (ego vehicle), through the control input

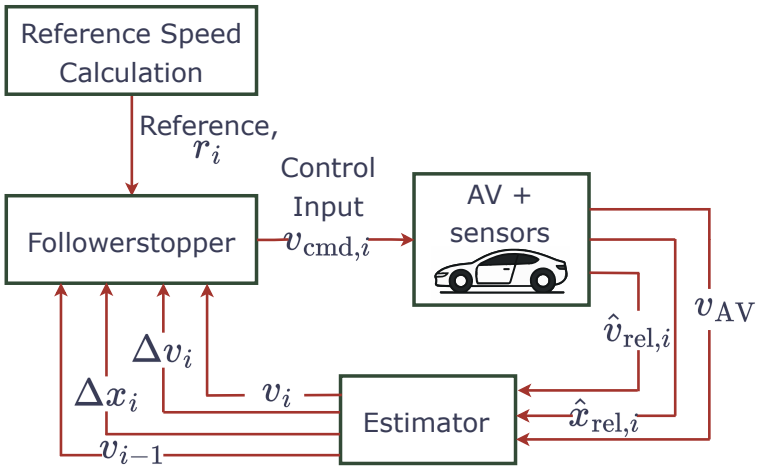

FIGURE 3: A block diagram showing Followerstopper used in our simulation experiment. Followerstopper control law, defined by Equation (1), acts as CACC in our work. In practice, each ego vehicle will need to estimate the relative distance and relative speed of its corresponding leader vehicle, which is represented using the **Estimator** block. However, in this work, relative distance and relative speed are assumed to be available.

u as shown in 3. One key requirement of Followerstopper is the reference input r_i, which is the desired free-flow speed if the vehicle doesn't encounter any leader vehicle within its sensor's range. How reference speed is calculated affects the behavior of Followerstopper. In Section 5.1, we describe the reference speed calculation for Followerstopper. However, readers are requested to refer to (*12*) for the algorithm used to calculate the reference in the original Arizona Ring-road Experiment (*8*, *9*). This formulation allows the ego vehicle to accelerate gradually as the headway increases, maintaining smooth transitions across modes. By controlling speed in this way, the Followerstopper controller reduces velocity perturbations and prevents sudden deceleration, which is critical for maintaining string stability (*8*, *12*).

String Stability Fundamentals

Definitions and Metrics

String stability ensures that disturbances such as speed fluctuations attenuate or at least do not amplify as they propagate downstream in a vehicle platoon. Consider a string of $n+1$ vehicles indexed by $i = 0, 1, 2, \ldots, n$, where $i = 0$ represents the lead vehicle. Strong string stability requires that

$$\sup_{t\geq 0} |\Delta v_i(t)| \leq \sup_{t\geq 0} |\Delta v_{i-1}(t)|, \quad \forall i \geq 1, \tag{4}$$

ensuring uniform boundedness of velocity differences. This is more restrictive than weak string stability, which requires attenuation only from the leader to the tail vehicle. Several metrics have been proposed in the literature to test for string stability. Among them, we focus on four widely accepted and complementary evaluation criteria for their theoretical rigor, interpretability, and practical relevance in both time and frequency domains (*18*–*20*).

Evaluation Criteria

$\mathscr{L}_2$-Norm-Based Time-Domain String Stability: String stability in the time domain can be evaluated by comparing the energy of relative velocity signals between successive vehicles. A widely adopted criterion based on the $\mathscr{L}_2$ norm ensures that disturbances in velocity do not amplify as they propagate downstream through the vehicle string. Formally, the system is said to be L_2 string stable if the following condition holds for all t:

$$\|v_{i+1}(t) - v_i(t)\|_2 \leq \|v_i(t) - v_{i-1}(t)\|_2, \tag{5}$$

where $\|\cdot\|_2$ denotes the L_2 norm, and $v_i(t)$ is the velocity of the i-th vehicle. This condition ensures that the energy of the velocity disturbance between any two consecutive vehicles does not increase as it propagates along the string. The use of the $\mathscr{L}_2$ norm provides a robust and interpretable framework for evaluating time-domain string stability, especially when frequency-domain transfer functions are difficult to estimate. A detailed discussion on $\mathscr{L}_p$-based string stability analysis, including $\mathscr{L}_2$, can be found in (*21*).

Head-to-Tail Amplification: This metric captures disturbance magnification from the leader (head) to the last follower (tail), defined as

$$A_{\text{ht}} = \max_t \frac{|v_n(t) - v_{\text{eq}}|}{|v_0(t) - v_{\text{eq}}|}, \tag{6}$$

where n is the last vehicle index. A string stable system requires $A_{\text{ht}} \leq 1$. It offers a global perspective, particularly useful in simulations and experimental studies (*20*).

Speed Disturbance Analysis: Speed disturbance quantifies the velocity difference between consecutive vehicles over time. It reflects how local speed perturbations amplify or dissipate along the platoon. A commonly used formulation is:

$$\Delta v_i(t) = v_{i-1}(t) - v_i(t), \tag{7}$$

where $v_i(t)$ is the velocity of the i-th vehicle at time t. Large or increasing values of $\Delta v_i(t)$ across vehicles are indicative of disturbance amplification and potential string instability. In contrast, reductions in $|\Delta v_i(t)|$ suggest effective damping or dissipation of the initial perturbation.

The concept aligns with the disturbance string stability framework introduced in the literature, which guarantees that perturbations in velocity tracking errors do not grow unbounded through the platoon under a delay-based spacing policy (*22*).

Relative speed profiles are particularly useful in distinguishing between manual and automated control phases. For instance, after the activation of a disturbance-aware controller such as the Follower-Stopper, the magnitude of relative speed oscillations tends to reduce significantly—demonstrating practical damping consistent with theoretical expectations.

The relative speed metric has been widely adopted in simulation- and field-based studies of string-stable platooning, serving as a time-domain indicator of disturbance propagation and qualitative controller performance.

Spacing Error Evaluation: Spacing error quantifies the deviation from desired inter-vehicle dis-

tance (*23*). A common form of spacing policy is:

$$d_i^{\text{des}}(t) = d_0 + hv_i(t), \tag{8}$$

where d_0 is a standstill distance and h is the time headway. The spacing error is defined as

$$e_i(t) = x_{i-1}(t) - x_i(t) - d_i^{\text{des}}(t). \tag{9}$$

String stability implies that $|e_i(t)|$ remains bounded or diminishes with increasing i.

Despite numerous proposed metrics, such as energy-based dissipation rates, $\mathscr{L}_2$ norms, or wave propagation speed, we adopt these metrics due to their complementary perspectives: local time response (time-domain metrics), system-wide attenuation (head-to-tail), and spacing regulation (spacing error). These criteria collectively provide comprehensive insights into both transient and steady-state behaviors, and they are widely used in (*18, 19, 24, 25*). This makes them robust tools for analyzing platoon stability across various modeling paradigms.

METHODOLOGY

We conducted a simulation consisting of one leader vehicle driven with an exogenous input taken from a real-world velocity profile, and seven automated vehicles controlled using Followerstopper that form a platoon and follow the leader. We assessed the string stability property of Followerstopper using two complementary simulations: SUMO and CARLA. At first, all the vehicles in the platoon were driving like humans using the IDM model, and then after 120 seconds, control was handed over to Followerstopper. IDM operation is necessary to see the utility of Followerstopper as a wave-dampening controller once the congestion is formed due to human driving behavior, simulated using IDM.

Experimental Setup

The experiment was conducted in a mixed-autonomy traffic scenario using both CARLA and SUMO simulators with the same initial setup. A total of eight vehicles were used, consisting of one leader and seven follower vehicles. The leader vehicle followed a real-world speed profile generated from CAN data (*26*), while all followers initially used the Intelligent Driver Model (IDM) for the first 120 s of the simulation. After this period, the followers switched to the Followerstopper (FS) controller to evaluate its ability to dampen traffic waves. For the FS controller, the reference speed was determined as the average of the leader's last 200 speed samples. During the simulation, we logged multiple parameters for each vehicle, including speed, longitudinal position, gap distance to the preceding vehicle, and relative speed, for later analysis of string stability.

Now, we describe the configuration used in SUMO and CARLA that we used for the simulation.

SUMO Setup: We used the SUMO simulator (version 1.23.1) to perform experiments in a straight highway configuration. The road consisted of a single-lane edge with a total length of 45 kilometers, generated using a custom ".net.xml" file. The simulation was run at a time step of 0.02 seconds (50 Hz).

The vehicle fleet included one leader and seven followers, all spawned at fixed intervals based on vehicle length (5m) and an initial gap of 4m. Vehicle types were defined using a custom "vType" in the ".rou.xml" file, including maximum acceleration, deceleration, and car-following model

settings. The initial configuration of the simulation scenario is illustrated in Fig. 4a, where one leader vehicle (shown in red) and multiple followers (depicted in distinct colors) are positioned along a single-lane straight highway with uniform spacing at standstill.

TraCI was used to monitor and update all vehicle states at each time step. The leader vehicle was controlled using real-world speed data applied at each step using the "traci.vehicle.setSpeed()" function. We recorded longitudinal position, speed, headway, inter-vehicle gap, and reference velocity for each vehicle. These data were later used for conducting string stability analysis.

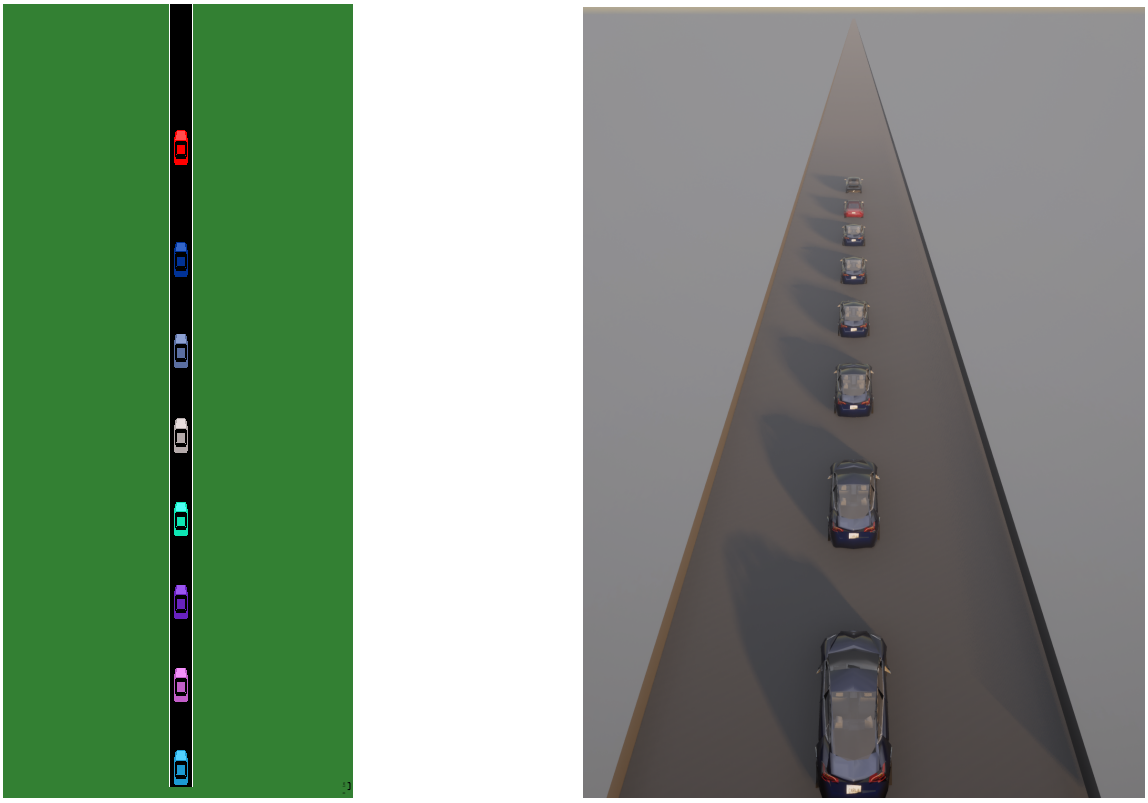

(a) Initial configuration in SUMO

(b) Initial configuration in CARLA

FIGURE 4: Initial configuration of the simulation scenario: (a) SUMO view displaying one leader (red) and multiple follower vehicles with distinct colors aligned on a straight highway, and (b) corresponding setup in CARLA. Vehicles are evenly spaced at standstill, serving as the starting condition for all control experiments.

CARLA Setup: The CARLA simulator (version 0.9.15) was run in synchronous mode to maintain deterministic behavior. The simulation was configured with a fixed tick rate of 50Hz, meaning the world updated every 0.02s. Vehicles were spawned on a custom OpenDRIVE-generated road network that was 45 km long, consisting of a single straight lane with a lane width of 4.5m to ensure no lane-changing behavior. Waypoint-following was used to keep the vehicles centered in the lane.

The initial platoon formation shown in Fig. 4b consisted of eight vehicles in total, arranged in a single-lane formation with one leader and seven follower vehicles. The leader vehicle was a Lincoln MKZ 2020, and the followers included one Audi TT (as the first follower) and six Tesla

Model 3 vehicles. Each vehicle was placed in the same lane with an initial gap of 4m between consecutive vehicles to ensure safe spacing at the start of the simulation. Data from the simulation was recorded using CARLA's Python API and saved for post-processing.

Leader Input Profile

The leader vehicle's speed trajectory(), shown in Fig. 5, was obtained from real-world CAN data and exhibits highly dynamic behavior over approximately 2200 seconds. The profile includes multiple acceleration and deceleration phases, rapid transitions, and several complete stops, which reflect realistic highway driving conditions with variable traffic flow. The speed signal was converted from kilometers per hour to meters per second and used as a time-dependent input in both SUMO and CARLA simulation environments.

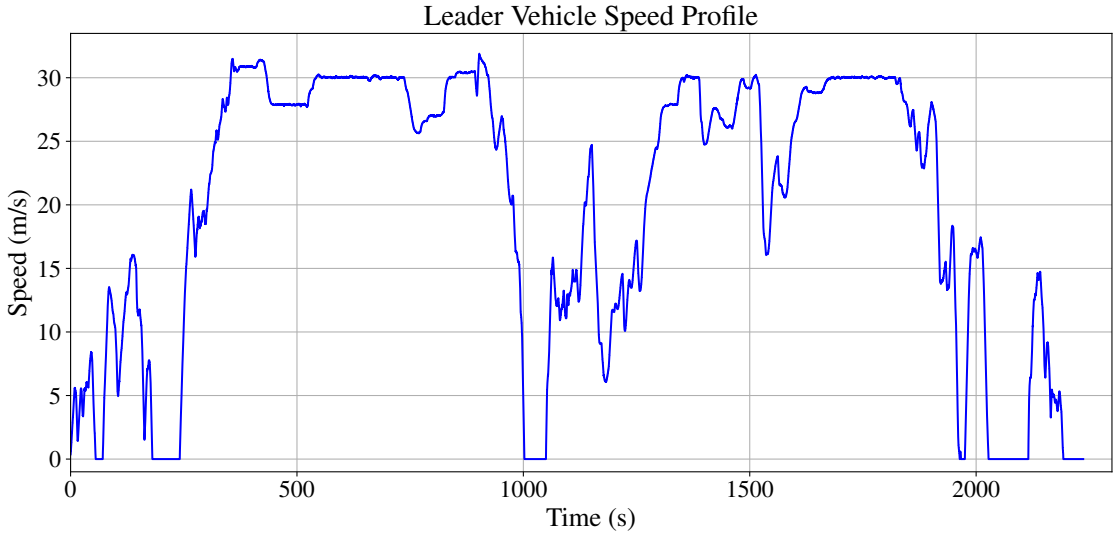

FIGURE 5: Leader vehicle velocity profile over time derived from real-world CAN data. The speed signal, originally recorded in km/h, was converted to m/s and plotted against time in seconds. This trajectory serves as the input for the leader in both SUMO and CARLA-based string stability simulations.

Formation of the Multi-Vehicle Platoon System

To investigate string stability and disturbance propagation in mixed-autonomy scenarios, we conduct a platoon experiment comprising eight vehicles. The first vehicle serves as the leader, driven by a prescribed velocity profile derived from real-world data. The remaining seven follower vehicles implement the Follower-Stopper (FS) controller within a simulation environment that assumes ideal sensing—i.e., no communication delay.

At each time t, let $v_i(t)$ denote the speed and $x_i(t)$ the longitudinal position of vehicle i. Each follower adheres to a constant-spacing policy, maintaining a desired inter-vehicle gap as defined in Eq. (8). The commanded speed $v_{\text{cmd},i}(t)$ is computed using Eq. (1), based on the spacing error and the relative velocity $\Delta v_i = v_{i-1}(t) - v_i(t)$.

Since SUMO does not model communication delay, all follower vehicles observe their immediate

predecessor's state without latency. This allows us to isolate and evaluate the FS controller's performance under delay-free conditions. The absence of vehicle-to-vehicle (V2V) delay simplifies the control update as follows:

$$v_i(t+\Delta t) \approx v_i^{\text{cmd}}(t), \tag{10}$$

subject to physical acceleration limits.

We evaluate string stability using four complementary metrics: (i) *L2-Norm-Based Time-Domain String Stability*, which measures the energy growth of inter-vehicle velocity differences; (ii) *Head-to-Tail Amplification*, which quantifies the maximum disturbance escalation from the leader to the last follower; (iii) *Speed Disturbance Analysis*, based on the time-varying relative velocity between adjacent vehicles; and (iv) *Spacing Error Evaluation*, which assesses deviations from its preceding vehicle.

This homogeneous eight-vehicle platoon configuration allows for controlled testing of string stability characteristics under ideal sensing conditions. The setup facilitates the direct assessment of the FS controller's ability to suppress disturbances without the confounding effects of communication latency. The following section presents simulation results from both SUMO and CARLA environments, with emphasis on pre- and post-controller activation behavior and the resulting impacts on string stability.

RESULT AND ANALYSIS

Simulation Results in SUMO and CARLA

Velocity Profile Analysis Under Human and Mixed-Autonomy Control

Figure-6 compares the vehicle speed trajectories in SUMO and CARLA simulations under two control conditions: fully human-driven (IDM) and mixed autonomy with the Follower–Stopper (FS) controller. Subplots 6a and 6c show the baseline scenario where all follower vehicles operate using the Intelligent Driver Model (IDM) throughout the simulation. Subplots 6b and 6d present the mixed-autonomy setting where IDM governs the platoon up to $t = 120\,\text{s}$, after which the FS controller is activated for all follower vehicles.

In the IDM-only case shown in (6a, 6c), disturbances in the leader's velocity propagate downstream, leading to increasingly speed fluctuations across follower vehicles. These oscillations are especially evident during acceleration and braking phases, where the trailing vehicles respond with lag and overshoot. The resulting speed profiles exhibit significant phase delay and magnitude amplification, characteristic of disturbance propagation in human-driven platoons.

By contrast, in the FS-enabled scenarios (6b, 6d), the follower speed trajectories become significantly smoother and more aligned after the controller activation. The FS controller mitigates the fluctuations seen in the IDM case, enabling faster convergence to the leader's speed profile and tighter coordination among followers.

Notably, around $t = 180\,\text{s}$, when the leader comes to a complete stop, the IDM-controlled followers exhibit delayed deceleration, with the last vehicle stopping nearly 20 s later. In the FS-controlled case, all follower vehicles decelerate more rapidly and reach zero velocity nearly simultaneously with the leader (around $t = 185\,\text{s}$), while preserving safe headway. This collective response demon-

strates the FS controller's ability to suppress stop-and-go behavior and enhance platoon stability. The improved velocity synchronization under FS control is consistent across both simulation platforms.

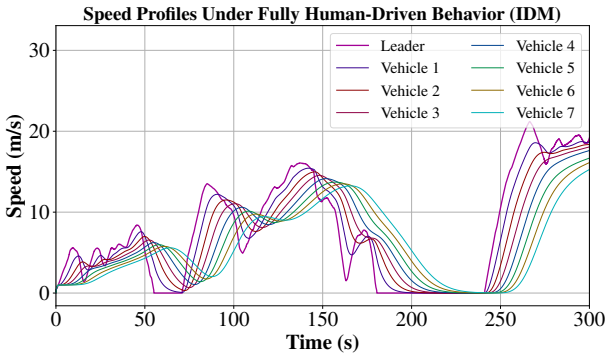

(a) SUMO: Fully Human-Driven Behavior (IDM)

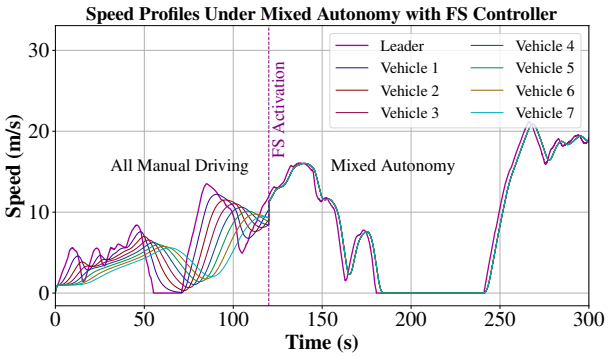

(b) SUMO: Mixed Autonomy (FS after $t = 120$ s)

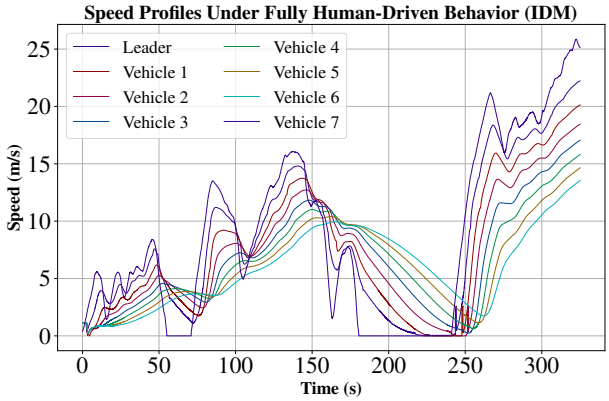

(c) CARLA: Fully Human-Driven Behavior (IDM)

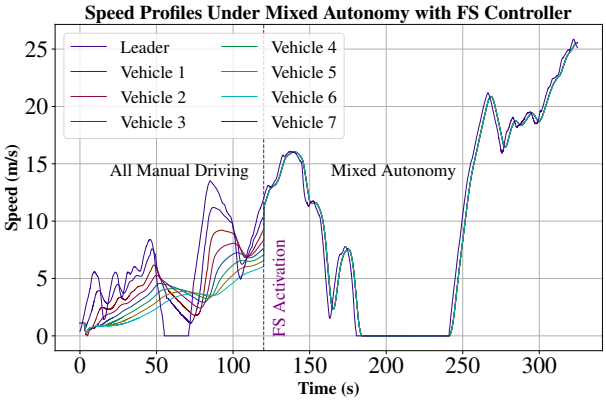

(d) CARLA: Mixed Autonomy (FS after $t = 120$ s)

FIGURE 6: Comparison of vehicle speed profiles simulated using SUMO and CARLA. In the left figures-(a) and (c), followers operate under the Intelligent Driver Model (IDM), representing fully human-driven behavior. In the right figure-(b) and (d), a mixed-autonomy setting is simulated: after $t = 120$s, all followers switch to the Followerstopper (FS) controller.

Analysis of Time–Space Diagram

The time–space heatmaps of vehicle speeds for two scenarios are shown in Figure-7: (a) fully human-driven behavior modeled using the IDM, and (b) mixed autonomy where the Follower–Stopper (FS) controller is activated after $t = 120$s. Each plot encodes vehicle trajectories over time, with speed $v_i(t)$ mapped to color.

In subplots 7a and 7c, the IDM-only scenario exhibits the spreading of trajectory curves and the widening of low-speed bands over time, indicating variations in velocity responses among vehicles. These patterns reflect a more dispersed speed distribution and suggest that disturbances are not uniformly regulated across the string.

Moreover, the overall flow recovery in the IDM case appears slower. Many vehicles remain in low-speed regimes for extended durations, as evidenced by the persistent red and yellow bands in the

heatmap. The mean flow speed in this scenario is approximately 12.83 m/s, indicating prolonged disturbance effects and inefficient speed recovery. In contrast, the FS-controlled platoon regains higher speeds more quickly and sustains them with greater consistency, resulting in a higher overall mean speed of 15.68 m/s. This highlights the controller's effectiveness in improving flow stability and reducing disturbance persistence across the platoon.

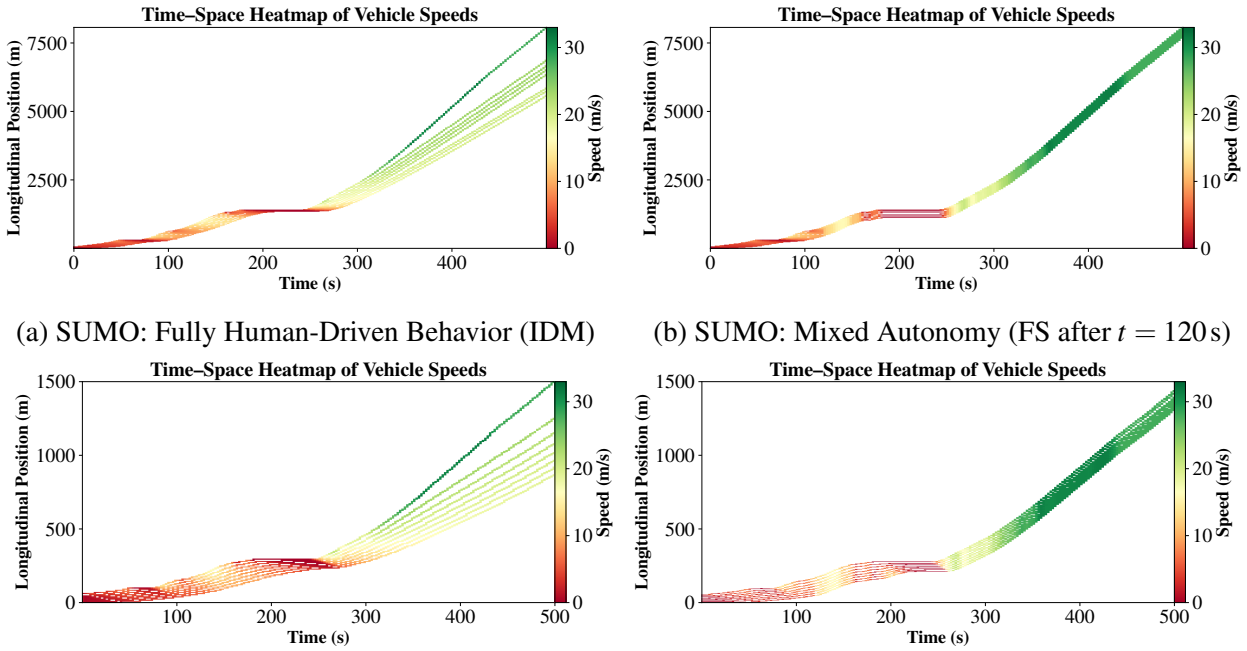

(a) SUMO: Fully Human-Driven Behavior (IDM)

(b) SUMO: Mixed Autonomy (FS after $t = 120\,\mathrm{s}$)

(c) CARLA: Fully Human-Driven Behavior (IDM)

(d) CARLA: Mixed Autonomy (FS after $t = 120\,\mathrm{s}$)

FIGURE 7: Time–space heatmaps of vehicle speeds simulated in (a) SUMO and (c) CARLA. Fully human-driven scenario where all vehicles are controlled using the Intelligent Driver Model (IDM). Mixed-autonomy scenario where all followers switch to the Followerstopper (FS) controller at $t = 120$s in (b) SUMO and (d) CARLA. The color encodes instantaneous vehicle speed, with red indicating lower speeds and green indicating higher speeds. The differences highlight the effect of autonomous control on traffic flow and disturbance dissipation.

Subplot 7b and 7d show the mixed-autonomy case. After FS activation at $t = 120\,\mathrm{s}$, vehicle trajectories become more aligned, and color bands stabilize across the platoon. This reflects reduced velocity fluctuations and disturbance attenuation. The consistency in spacing also suggests that the spacing error $e_i(t)$ remains bounded post-activation and indicates effective headway regulation. This visual shows the controller's effectiveness in damping both speed and spacing disturbances in a delay-free setting.

String Stability Testing

$\mathscr{L}_2$-Norm Evaluation of Relative Velocity Disturbances

We adopt the widely used $\mathscr{L}_2$ norm approach to evaluate string stability in the time domain by assessing the disturbances of relative velocity between vehicles that are attenuated as they propa-

gate downstream. Figure-8 illustrates the $\mathscr{L}_2$ norms of relative velocities $\Delta v_i(t)$ for each vehicle in both SUMO and CARLA simulations. In subplot 8a and subplot 8b, the purple bars represent $\|v_i(t) - v_{i-1}(t)\|_2$ and the green bars correspond to $\|v_{i+1}(t) - v_i(t)\|_2$. Across all follower positions, the green bars are consistently lower than the preceding purple bars, indicating that the inequality in Eq-5 is satisfied throughout the platoon. This suggests that velocity disturbances decay downstream under the Followerstopper controller.

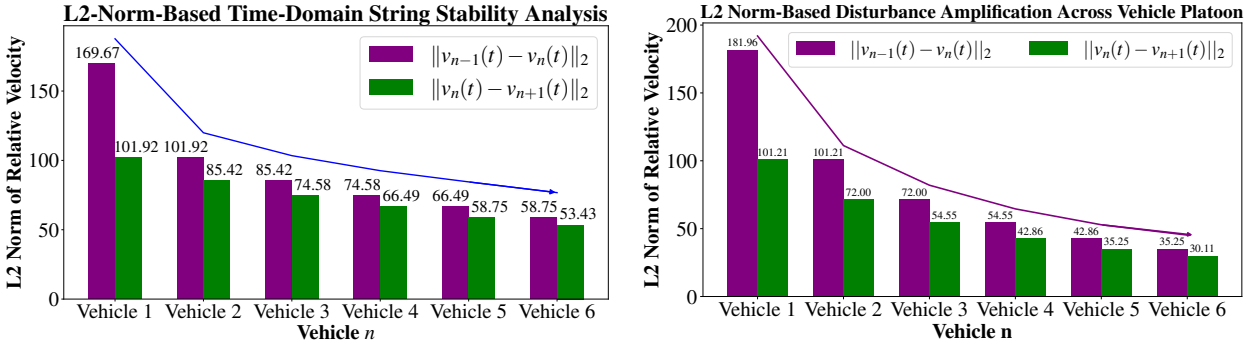

(a) SUMO: $\mathscr{L}_2$ Norms of Relative speed $\Delta v_i(t) = v_{i-1}(t) - v_i(t)$ between successive vehicles

(b) CARLA: $\mathscr{L}_2$ Norms of Relative speed $\Delta v_i(t) = v_{i-1}(t) - v_i(t)$ between successive vehicles

FIGURE 8: Time-domain string stability analysis using $\mathscr{L}_2$ norms of relative velocity between successive vehicles. The condition $\|v_{n+1}(t) - v_n(t)\|_2 \leq \|v_n(t) - v_{n-1}(t)\|_2$ ensures that speed disturbances do not amplify downstream. Both (a) SUMO and (b) CARLA simulations show that this condition is satisfied under the Followerstopper controller.

A similar trend is observed in subplot 8b for CARLA-based experiments. While absolute $\mathscr{L}_2$ values vary slightly due to differences in vehicle dynamics and simulation fidelity, the qualitative pattern of decreasing relative velocity energy persists. This consistency between two independent platforms indicates the robustness of the Followerstopper control policy in maintaining $\mathscr{L}_2$-based string stability.

Overall, the steady decrease in $\mathscr{L}_2$ norms across vehicles shows that the platoon gradually reduces speed disturbances. This confirms that the energy-based string stability condition is satisfied and that the system maintains good coordination in both realistic and ideal simulation setups.

Head-to-Tail Amplification Test

To evaluate string stability from a head-to-tail perspective, we compute the amplification ratio using Eq.6. In our SUMO-based simulation, the equilibrium velocity was computed as $V_{eq} = 15.68\,\text{m/s}$, and the resulting amplification ratio was $A_t = 0.994$. A similar value was observed in CARLA. Since $A_t \leq 1$ in both cases, the platoon satisfies the head-to-tail string stability condition. This indicates that the Followerstopper controller prevents the amplification of velocity disturbances at the tail end of the platoon.

Relative Speed and Space Headway Disturbance Analysis

To assess the propagation of disturbances along the platoon, we analyze two closely related metrics: relative speed $\Delta v_i(t)$ and space headway $\Delta x_i(t)$. Both indicate how a vehicle responds to its leader vehicle in terms of velocity and spacing, respectively, and serve as useful indicators of local string stability.

Figure 9 presents the relative speed profiles for all followers in SUMO and CARLA simulations. During the IDM-only phase, significant fluctuations in $\Delta v_i(t)$ are observed, particularly in downstream vehicles. This suggests that velocity disturbances from the leader amplify as they propagate, causing non-uniform behavior in the platoon. After the Followerstopper (FS) controller is activated, these fluctuations are quickly reduced, and the relative speeds across vehicles become more synchronized and centered around zero. This damping effect is consistently observed in both simulation platforms.

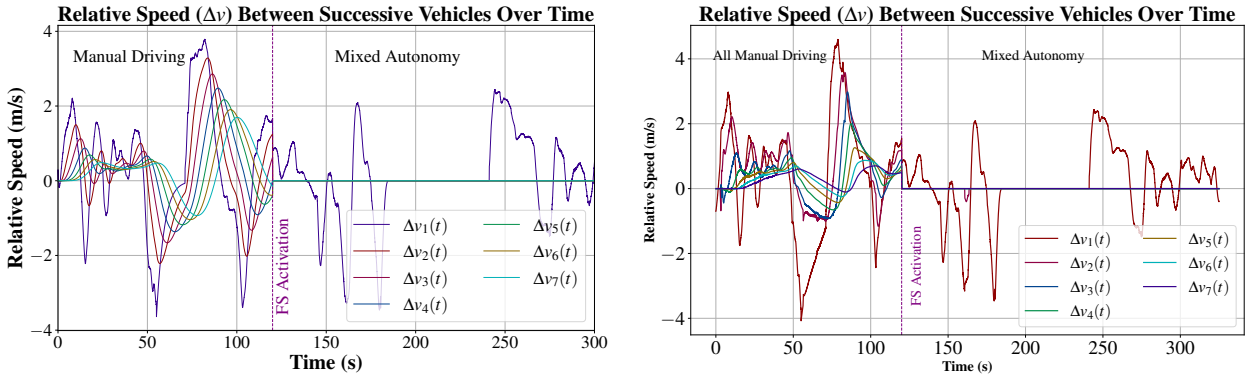

(a) SUMO: Relative speed $\Delta v_i(t) = v_{i-1}(t) - v_i(t)$ between successive vehicles

(b) CARLA: Relative speed $\Delta v_i(t) = v_{i-1}(t) - v_i(t)$ between successive vehicles

FIGURE 9: Relative speed profiles $\Delta v_i(t)$ between successive vehicles in manual and mixed autonomy settings. Disturbance amplification under manual control is mitigated after the Followerstopper controller is applied.

Similarly, Figure 10 shows the changes over time of space headway $\Delta x_i(t)$. In the manual driving phase, both SUMO and CARLA simulations exhibit noticeable oscillations in spacing between vehicles, which tend to increase with vehicle index. These irregular spacing patterns are a typical characteristic of human-driven car-following behavior, where drivers respond reactively rather than proactively. After FS activation, space headway curves flatten out, and vehicles maintain consistent gaps. SUMO followers converge to stable spacing around 35–40 meters, while CARLA simulations show a similar trend on a slightly smaller scale.

In both cases, the FS controller effectively suppresses disturbances in relative speed and spacing. The convergence of $\Delta v_i(t)$ and $\Delta x_i(t)$ trajectories indicates better coordination, reduced stop-and-go behavior, and improved platoon coherence. Moreover, the bounded nature of the spacing error $e_i(t)$ shows the system's adherence to string stability requirements. These consistent outcomes across different simulators indicate the robustness of the FS controller in managing inter-vehicle dynamics in both ideal and realistic simulation environments.

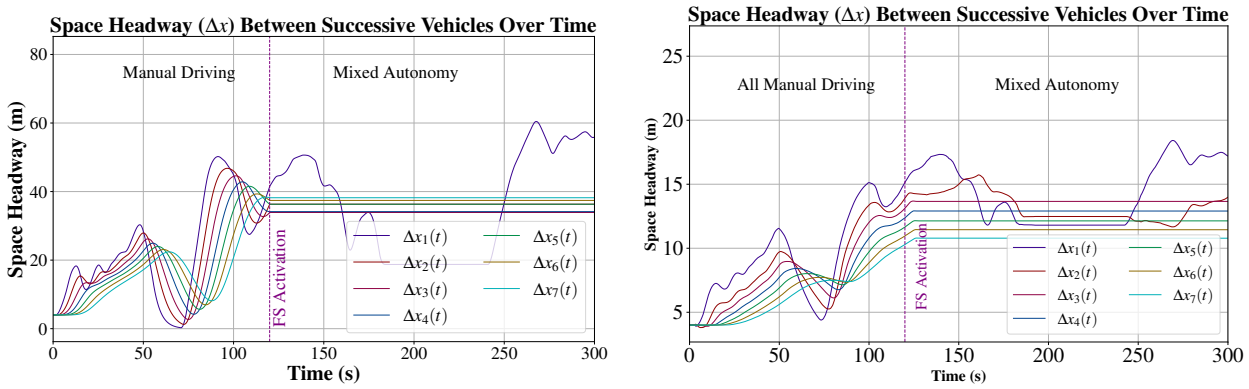

(a) SUMO: Space headway disturbance

(b) CARLA: Space headway disturbance

FIGURE 10: Space headway disturbances between successive vehicles under manual and mixed autonomy scenarios. Each curve represents the space headway $\Delta x_i(t)$ between vehicle $i-1$ and i. After FS activation at $t = 120\,\text{s}$, space headways stabilize.

CONCLUSION

This study examined the string stability characteristics of an eight-vehicle platoon controlled using the Followerstopper (FS) controller under realistic and idealized simulation conditions. Using real-world leader velocity profiles as input, we conducted parallel experiments in SUMO and CARLA to assess how velocity and spacing disturbances propagate through the platoon.

The results demonstrate that the FS controller effectively suppresses stop-and-go waves and attenuates velocity mismatches, as evidenced by reduced fluctuations in relative speed and space headway. Time-domain string stability was validated through several complementary metrics, including head-to-tail amplification, $\mathscr{L}_2$ norm-based disturbance energy, and bounded spacing error. In all cases, disturbances were shown to dissipate downstream, confirming the FS controller's ability to regulate inter-vehicle dynamics and maintain coherent platoon formation.

Both simulation environments consistently showed post-controller improvements in flow stability, coordination, and spacing uniformity. These findings reinforce the viability of the FS controller as a disturbance-aware strategy for mitigating traffic oscillations in mixed-autonomy scenarios.

Future work may extend this framework to incorporate communication delays, heterogeneous vehicle models, and real-time deployment to further validate performance under broader traffic conditions.

REFERENCES

1. Chen, L., P. Wu, K. Chitta, B. Jaeger, A. Geiger, and H. Li, End-to-end autonomous driving: Challenges and frontiers. *IEEE Transactions on Pattern Analysis and Machine Intelligence*, 2024.
2. Snyder, R., Implications of autonomous vehicles: A planner's perspective. *Institute of Transportation Engineers. ITE Journal*, Vol. 86, No. 12, 2016, p. 25.
3. Pan, Y., Y. Wu, L. Xu, C. Xia, and D. L. Olson, The impacts of connected autonomous vehicles on mixed traffic flow: A comprehensive review. *Physica A: Statistical Mechanics and its Applications*, Vol. 635, 2024, p. 129454.
4. Tigadi, A., R. Gujanatti, A. Gonchi, and B. Klemsscet, Advanced driver assistance systems. *International Journal of Engineering Research and General Science*, Vol. 4, No. 3, 2016, pp. 151–158.
5. Ishida, S. and J. E. Gayko, Development, evaluation and introduction of a lane keeping assistance system. In *IEEE Intelligent Vehicles Symposium, 2004*, IEEE, 2004, pp. 943–944.
6. Xiao, L. and F. Gao, A comprehensive review of the development of adaptive cruise control systems. *Vehicle system dynamics*, Vol. 48, No. 10, 2010, pp. 1167–1192.
7. Gunter, G., D. Gloudemans, R. E. Stern, S. McQuade, R. Bhadani, M. Bunting, M. L. Delle Monache, R. Lysecky, B. Seibold, J. Sprinkle, et al., Are commercially implemented adaptive cruise control systems string stable? *IEEE Transactions on Intelligent Transportation Systems*, Vol. 22, No. 11, 2020, pp. 6992–7003.
8. Stern, R. E., S. Cui, M. L. Delle Monache, R. Bhadani, M. Bunting, M. Churchill, N. Hamilton, R. Haulcy, H. Pohlmann, F. Wu, et al., Dissipation of stop-and-go waves via control of autonomous vehicles: Field experiments. *Transportation research part C: emerging technologies*, Vol. 89, 2018, pp. 205–221.
9. Bhadani, R. K., B. Piccoli, B. Seibold, J. Sprinkle, and D. Work, Dissipation of emergent traffic waves in stop-and-go traffic using a supervisory controller. In *2018 IEEE Conference on Decision and Control (CDC)*, IEEE, 2018, pp. 3628–3633.
10. Lee, J. W., H. Wang, K. Jang, N. Lichtlé, A. Hayat, M. Bunting, A. Alanqary, W. Barbour, Z. Fu, X. Gong, et al., Traffic control via connected and automated vehicles (cavs): An open-road field experiment with 100 cavs. *IEEE Control Systems*, Vol. 45, No. 1, 2025, pp. 28–60.
11. Bayen, A. M., J. W. Lee, B. Piccoli, B. Seibold, J. M. Sprinkle, and D. B. Work, *CIRCLES: Congestion impacts reduction via CAV-in-the-loop Lagrangian energy smoothing*. University of California, Berkeley, CA (United States), 2024.
12. Bhadani, R., Followerstopper Revisited: Phase-space Lagrangian Controller for Traffic Decongestion. *arXiv preprint arXiv:2506.08036*, 2025.
13. Wang, Z., G. Wu, and M. J. Barth, A review on cooperative adaptive cruise control (CACC) systems: Architectures, controls, and applications. In *2018 21st International Conference on Intelligent Transportation Systems (ITSC)*, IEEE, 2018, pp. 2884–2891.
14. Krajzewicz, D., Traffic simulation with SUMO–simulation of urban mobility. In *Fundamentals of traffic simulation*, Springer, 2010, pp. 269–293.
15. Dosovitskiy, A., G. Ros, F. Codevilla, A. Lopez, and V. Koltun, CARLA: An open urban driving simulator. In *Conference on robot learning*, PMLR, 2017, pp. 1–16.

16. Hu, J., S. Sun, J. Lai, S. Wang, Z. Chen, and T. Liu, CACC simulation platform designed for urban scenes. *IEEE Transactions on Intelligent Vehicles*, Vol. 8, No. 4, 2023, pp. 2857–2874.
17. Sugiyama, Y., M. Fukui, M. Kikuchi, K. Hasebe, A. Nakayama, K. Nishinari, S.-i. Tadaki, and S. Yukawa, Traffic jams without bottlenecks—experimental evidence for the physical mechanism of the formation of a jam. *New journal of physics*, Vol. 10, No. 3, 2008, p. 033001.
18. Zhang, Y., Z. Xu, Z. Wang, X. Yao, and Z. Xu, Impacts of communication delay on vehicle platoon string stability and its compensation strategy: A review. *Journal of traffic and transportation engineering (English edition)*, Vol. 10, No. 4, 2023, pp. 508–529.
19. Gratzer, A. L., S. Thormann, A. Schirrer, and S. Jakubek, String stable and collision-safe model predictive platoon control. *IEEE Transactions on Intelligent Transportation Systems*, Vol. 23, No. 10, 2022, pp. 19358–19373.
20. Mokogwu, C. N. and K. Hashtrudi-Zaad, Energy-based analysis of string stability in vehicle platoons. *IEEE Transactions on Vehicular Technology*, Vol. 71, No. 6, 2022, pp. 5915–5929.
21. Ploeg, J., N. Van De Wouw, and H. Nijmeijer, Lp string stability of cascaded systems: Application to vehicle platooning. *IEEE Transactions on Control Systems Technology*, Vol. 22, No. 2, 2013, pp. 786–793.
22. Besselink, B. and K. H. Johansson, String Stability and a Delay-Based Spacing Policy for Vehicle Platoons Subject to Disturbances. *IEEE Transactions on Automatic Control*, Vol. 62, No. 9, 2017, pp. 4376–4391.
23. Petrinić, T. and I. Petrović, Longitudinal spacing control of vehicles in a platoon for stable and increased traffic flow. In *2012 IEEE International Conference on Control Applications*, IEEE, 2012, pp. 178–183.
24. Feng, S., Y. Zhang, S. E. Li, Z. Cao, H. X. Liu, and L. Li, String stability for vehicular platoon control: Definitions and analysis methods. *Annual Reviews in Control*, Vol. 47, 2019, pp. 81–97.
25. Devika, K., G. Rohith, V. R. S. Yellapantula, and S. C. Subramanian, A dynamics-based adaptive string stable controller for connected heavy road vehicle platoon safety. *IEEE Access*, Vol. 8, 2020, pp. 209886–209903.
26. Bunting, M., R. Bhadani, M. Nice, S. Elmadani, and J. Sprinkle, Data from the development evolution of a vehicle for custom control. In *2022 2nd Workshop on Data-Driven and Intelligent Cyber-Physical Systems for Smart Cities Workshop (DI-CPS)*, IEEE, 2022, pp. 40–46.